



Global Vertical Distribution of Water Vapor in the Martian Atmosphere for 6 years of ExoMars-TGO/NOMAD observations.

A. Brines¹, M.A. Lopez-Valverde¹, B. Funke¹, F.G. Galindo¹, A. Modak^{1,8}, A. Stolzenbach¹, J.J. Lopez-Moreno¹, R.M. Sanz-Mesa¹, S. Aoki^{2,3}, A.C. Vandaele², F. Daerden², I.R. Thomas², J.T. Erwin², L. Trompet², B. Ristic², G.L. Villanueva⁴, G. Iuzzi⁵, M.R. Patel⁶, G. Bellucci⁷, and the NOMAD team

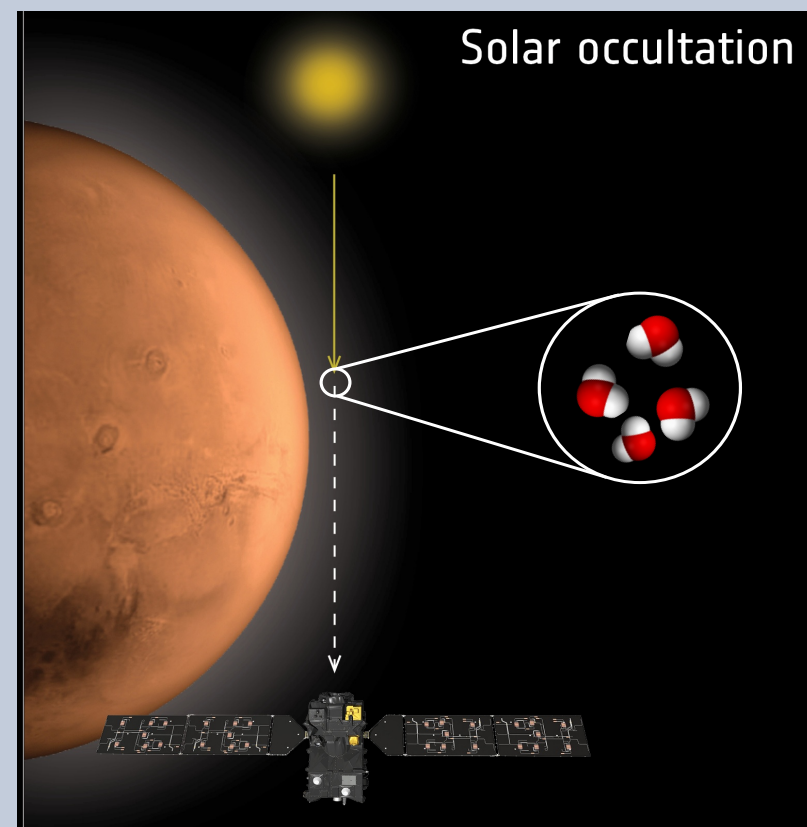
¹Instituto de Astrofísica de Andalucía (IAA/CSIC), Spain; ²Royal Belgian Institute for Space Aeronomy, Belgium; ³Department of Complexity Science and Engineering, University of Tokyo, Japan; ⁴NASA Goddard Space Flight Center, USA; ⁵University of Basilicata, Italy; ⁶Open University, UK; ⁷Istituto di Astrofisica e Planetologia, Italy; ⁸Institute for Basic Science, South Korea



1. Motivation

The characterization of the water vapor vertical distribution on Mars is currently a very active research topic. Until this last decade, the water cycle has been studied mainly with the analysis of column density abundances. The addition of Solar Occultation (SO) observations with the ExoMars Trace Gas Orbiter (TGO) mission has opened a new path towards a better understanding of the Martian climate [1].

The Mars we observe today is a **dry and cold** planet, although there are abundant evidences suggesting a warmer and wetter environment in the past [2]. Despite being a minor species in the current Martian atmosphere (~0.03%), water vapor has a **large variability** throughout the year, resulting in a very complex **hydrological cycle** involving sublimation and condensation processes affected by dust and atmospheric transport [1].



We present here the recent results of [3], [4] devoted to characterize the water vapor in the Martian atmosphere with vertical profiles up to 120 km altitude. In **Section 2** we present the **NOMAD instrument** and the data analysis **methodology**. In **Section 3** we study the water vapor **latitudinal distribution** during **3 Martian Years** (MYs 34, 35 and 36). We analyze 1065 NOMAD SO observations during specific L_s periods, showing the effects of a strong localized vertical transport injecting water vapor into high altitudes. In **Section 4** we show its **interannual variability**. In **Section 5** we provide an estimation of the **hydrogen escape** to space. The main **conclusions** are summarized in **Section 6**.

Fig. 1: Schematic of Solar Occultation geometry

3. Latitudinal Distribution

We selected observations during and after the **perihelion season**, covering three similar L_s ranges. The latitudinal distribution of H_2O is presented in Fig. 5. We have binned the retrieved profiles in 5° latitude intervals considering each profile's uncertainty.

During these L_s periods, we observed a **vertical column of H_2O** (denoted as "**plume**") with abundance about **50 ppmv** at $60^\circ S - 30^\circ S$ reaching altitudes up to **100 km** during L_{s2} in MYs 35 and 36 (Fig. 5-B2, 5-C2). MY 34 also showed a similar structure but with reduced abundance and with a peak showing up later in the season.

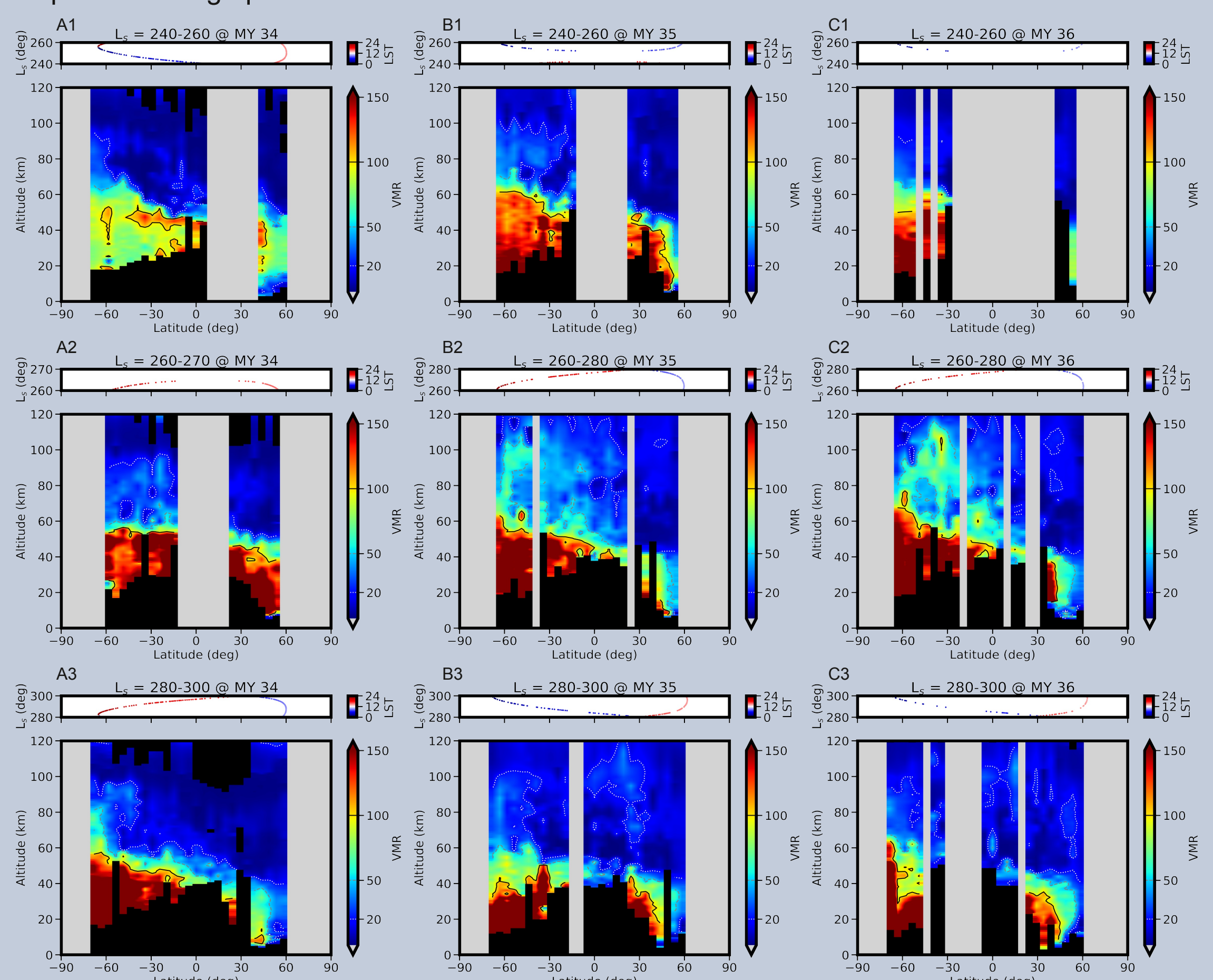


Fig. 5: Water vapor latitudinal variation during $L_{s1}=240^\circ - 260^\circ$ (A1, B1, C1), $L_{s2}=260^\circ - 280^\circ$ (A2, B2, C2) and $L_{s3}=280^\circ - 300^\circ$ (A3, B3, C3) for MYs 34 (left), 35 (middle) and 36 (right). Lines show VMR contours at 100 (black), 50 (gray) and 20 (white) ppmv. Dots in panels A1-A3, B1-B3, C1-C3 indicate the latitude, Solar Longitude and Local Solar Time of the observations.

5. Hydrogen escape

We estimated the **hydrogen escape flux** induced by the observed water vapor plume using the approximated method by [17]. We have averaged all the vertical profiles in the southern hemisphere for latitudes above 45 degrees during the three L_s periods ($L_{s1} = 240^\circ - 260^\circ$, $L_{s2} = 260^\circ - 280^\circ$ and $L_{s3} = 280^\circ - 300^\circ$) for each MY, as shown in Figure 6. The total contribution to the hydrogen escape for each MY and L_s period is presented in Figure 7. We obtained an integral escape flux associated to the plumes of about $\sim 3.2 \pm 0.5 \times 10^9 \text{ cm}^{-2} \text{ s}^{-1}$, which is in a similar range as previous results [18], [19], [20].

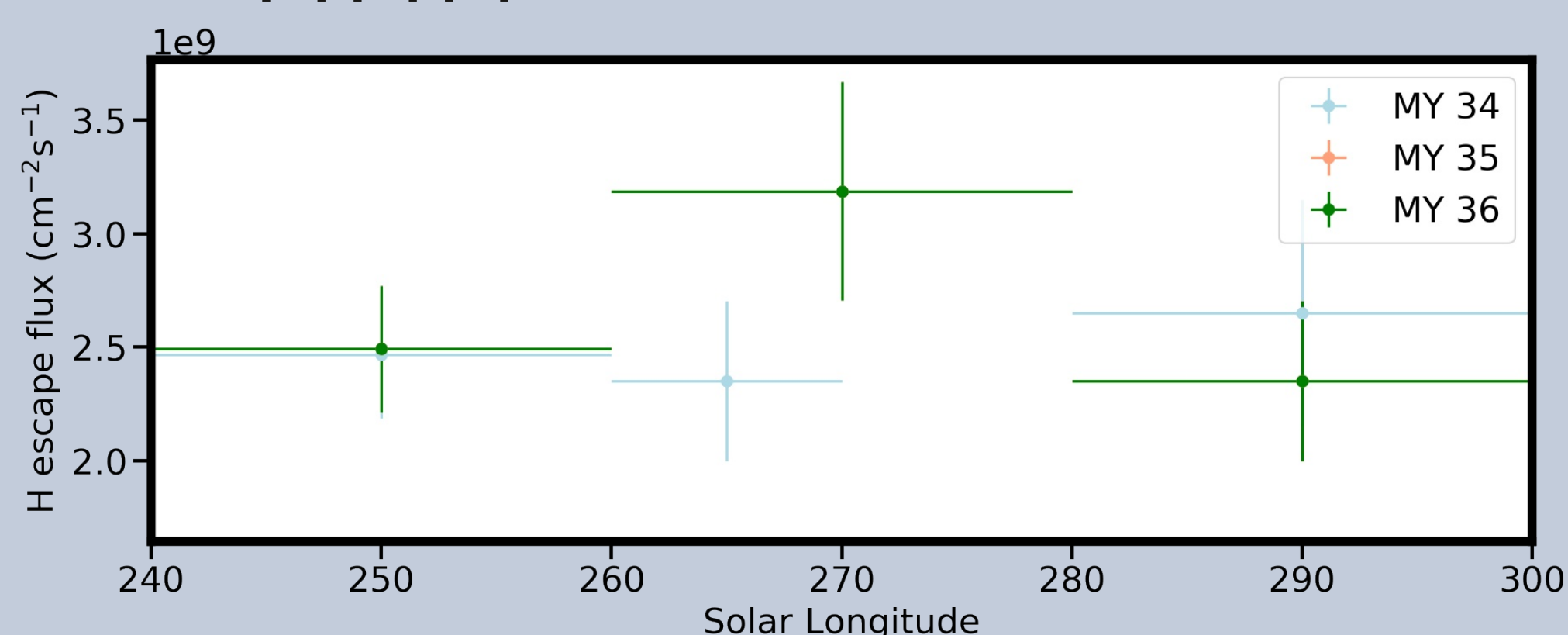


Fig. 7: estimated hydrogen flux for MYs 34 (light blue), 35 (orange) and 36 (green). Note that orange and green points are overlapped.

This flux represents a modest but not negligible **increase**, marginally above our uncertainties of **30±25%** compared to our estimation of the escape for the periods when the plume was not detected.

References

- [1] MONTMESSIN, Franck et al., 2017
- [2] BIBRING, Jean-Pierre et al., 2006
- [3] BRINES, Adrian et al., 2024a
- [4] BRINES, Adrian, PhD Thesis, 2024b
- [5] VANDAELE, Ann Carine et al., 2018
- [6] BRINES, Adrian et al., 2022
- [7] LÓPEZ-VALVERDE, Miguel Angel et al., 2023
- [8] MODAK, Ashimananda et al., 2023
- [9] STOLZENBACH, Aurélien et al., 2023
- [10] BRINES, Adrian et al., 2024c (this conference)
- [11] GONZALEZ-GALINDO, Francisco 2024 (this conference)
- [12] MODAK, Ashimananda et al., 2024 (this conference)
- [13] THOMAS, Ian R. et al., 2022
- [14] TROMPET, Loïc et al., 2023
- [15] STILLER, G. P., 2000
- [16] VILLANUEVA, Geronimo L. et al., 2022
- [17] CHAFFIN, M. S. et al., 2017
- [18] BELYAEV, Denis et al., 2021
- [19] BHATTACHARYYA, D. et al., 2017
- [20] HOLMES, James et al., 2021
- [21] STREETER, Paul et al., 2021
- [22] GUNDLACH, B. et al., 2011

2. NOMAD and Data Analysis

NOMAD is an infrared spectrometer covering the spectral range between 0.2 to 4.3 μm . Its SO channel uses an Echelle grating with with an Acousto-Optical Tunable Filter (AOTF) to select different diffraction orders to be used during the observations. The spectral resolution of the SO channel is $\lambda/\Delta\lambda = 17,000$. The sampling allows a **vertical resolution of about 2-10 km**. Also, the AOTF permits probing the atmosphere at a given altitude through 6 different diffraction orders [5].

In addition to the **water vapor** [3], [4], [6], our processing pipeline has been optimized to retrieve **temperature** [7], **carbon monoxide** [8] and **aerosol** [9] vertical profiles, providing a wide overview of the Martian atmosphere. **Companion posters** showing the global vertical distribution of HCl [10], temperature variability [11] and CO vertical profiles [12] are also presented in this conference.



Fig. 2: The NOMAD instrument with its Solar Occultation (SO), Limb/Nadir Observation (LNO) and UV-visible (UVIS) channels.

For this study, we use Level 1 SO calibrated **transmittances** [13], [14] of diffraction orders **134** ($3011-3035 \text{ cm}^{-1}$), **136** ($3056-3081 \text{ cm}^{-1}$) for the lower atmosphere below 60 km, and **168** ($3775-3806 \text{ cm}^{-1}$), **169** ($3798-3828 \text{ cm}^{-1}$) for the upper atmosphere above 60 km.

We have developed **pre-processing** tools to identify and eliminate residual artifacts in the spectra (bending, spectral shift) using the **line-by-line radiative transfer** algorithm KOPRA [15]. During the inversions, we implemented into our Forward Model the latest calibration of the NOMAD AOTF and its instrumental line-shape (ILS) [16]. The **retrievals** are done **combining** the spectra of **high altitude** orders (134, 136) with spectra of **low altitude** orders (168, 169) up to **120 km** for occultations where those orders were observed simultaneously.

Fig. 4: Typical water vapor vertical profile (blue) obtained after the inversion of a NOMAD SO atmospheric scan. Green dashed line shows the a priori atmosphere.

The best fit obtained during the inversion is good. This is illustrated in Fig. 3 with two examples of typical NOMAD spectra (black) after its bending and spectral shift corrections for diffraction orders 136 (panel A) and 169 (panel B) at 30 and 100 km respectively. We also show the fitting after the retrieval (red). For optimization purposes, we only fit the data at certain spectral windows where the strongest H_2O absorption lines are located. The panel on the bottom shows a typical retrieved H_2O vertical profile (solid blue) and the GCM a priori used during its inversion (dashed green).

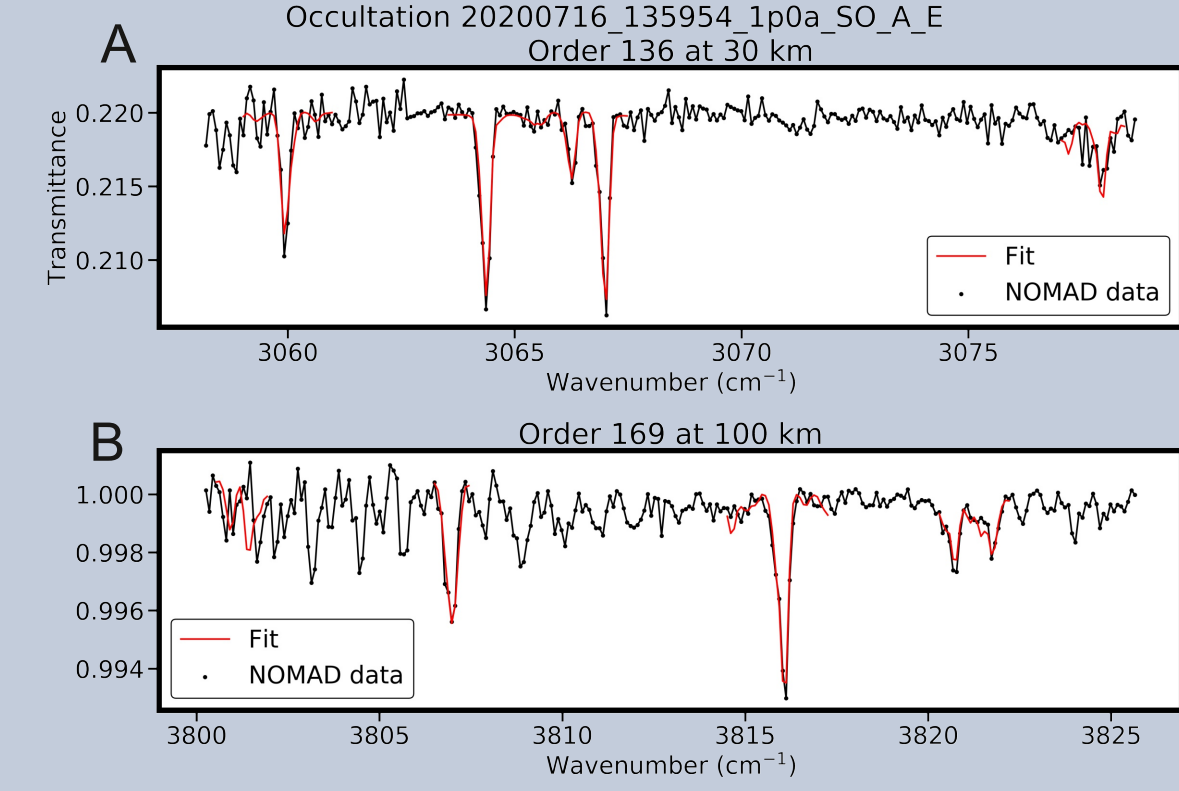
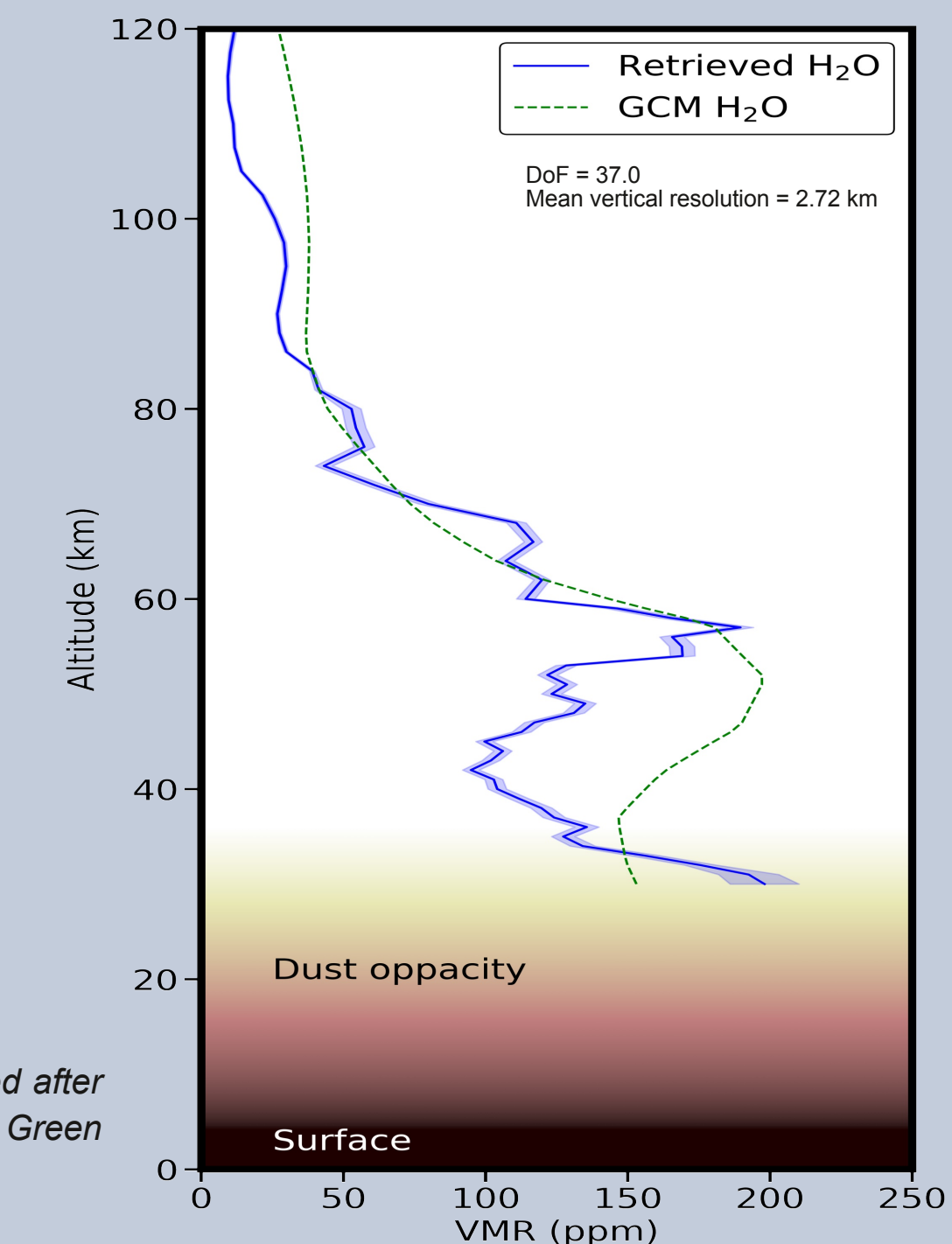


Fig. 3: NOMAD SO spectra (black) from diffraction orders 136 at 30 km altitude (panel A) and 169 at 100 km altitude (panel B). Red line shows the best fit of the forward model at the water vapor absorption lines obtained during the retrieval.



4. Interannual Variability

We averaged the retrieved profiles within the solar longitude ranges L_{s1} , L_{s2} and L_{s3} for each analyzed MY, excluding observations from latitudes between the equator and 45° in order to capture only vertical profiles **representative of the observed plume** during each MY. The average H_2O profiles for each L_s range in the southern hemisphere are presented in Fig. 6 for MYs 34 (A), 35 (B) and 36 (C). The difference in ppmv between L_{s2} and L_{s3} profiles is shown in panel D. We observed a clear **enhancement** of the water abundance above 80 km of about 30 ppmv during L_{s2} in MYs 35 and 36 (orange and green lines), showing a similar vertical structure in both years. In contrast, MY 34 shows an enhancement of only 15 ppmv during L_{s3} .

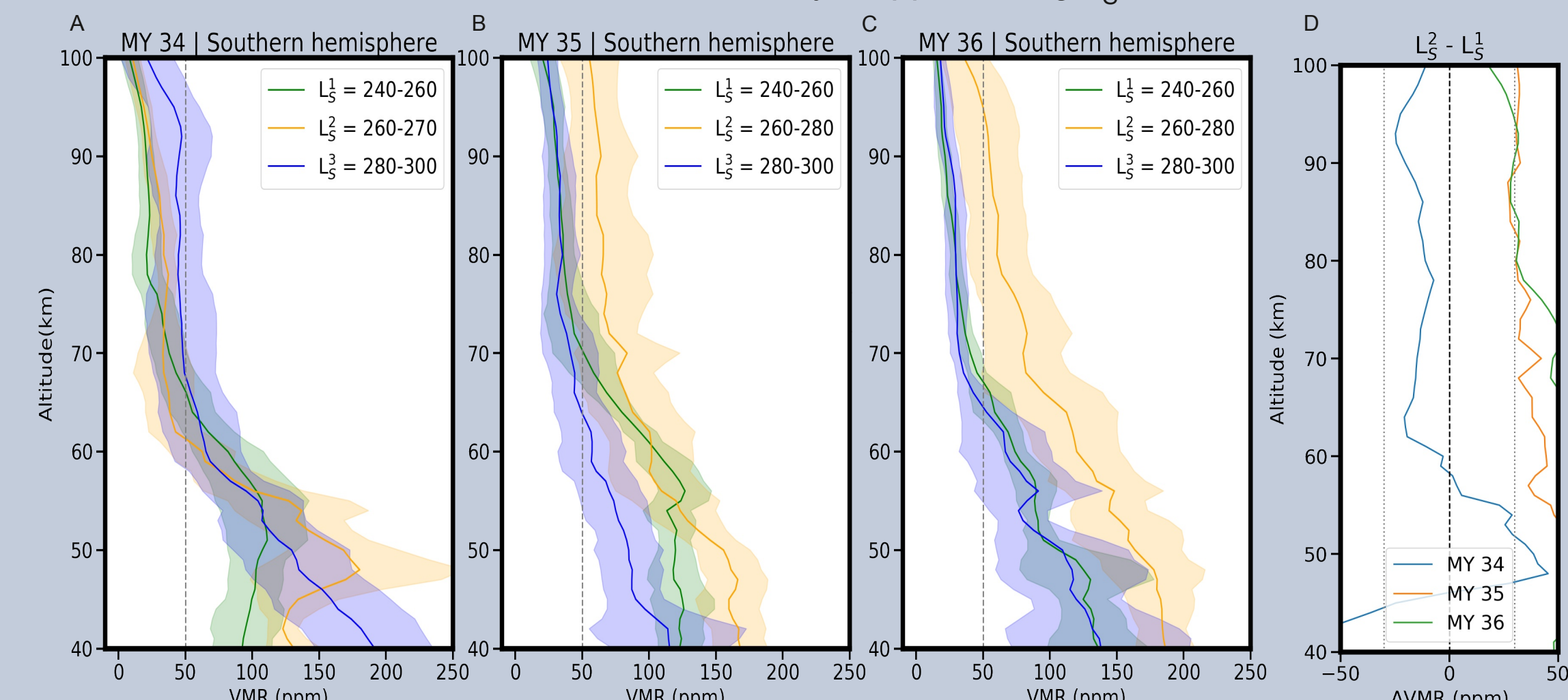


Fig. 6: Averaged water vapor VMR profiles at southern hemisphere during solar longitude ranges $L_{s1} = 240^\circ - 260^\circ$ (A), $L_{s2} = 260^\circ - 280^\circ$ (B) and $L_{s3} = 280^\circ - 300^\circ$ (C) for MYs 34 (A), 35 (B), and 36 (C). Profiles from latitudes below 45° have been excluded in the average. Shaded areas represent the standard deviation of the average. Vertical dashed lines indicate abundance of 50 ppmv. Panel D shows the averaged profiles difference $L_{s2}-L_{s3}$ for MYs 34 (blue), 35 (orange) and 36 (green). Vertical dotted lines indicate abundance of 30 ppmv (dotted) and 0 ppmv (dashed) for reference.

6. Conclusions

This study focuses on the vertical distribution of water vapor during **perihelion** and **southern summer solstice**. We have obtained ~ 1000 H_2O profiles from the lower troposphere up to 120 km altitude, with a vertical resolution of 2-10 km. The latitudinal variations over 3 MYs reveal the presence of water vapor in **significant amounts** in the **upper mesosphere**, as it is transported vertically at **60°S - 50°S**. The main **conclusions** of this study can be summarized as follows:

- The latitudinal distribution seems to agree with climate model predictions for the time of year studied here but shows a clear **plume at mesospheric altitudes**.
- This water vapor plume occurs for a **short period** (20° in L_s) but **repeats during three Martian years** (MYs), with a clear **interannual variability**.
- During **non-global dust storm years** (MYs 35 and 36), the water vapor injection occurs at $L_s = 260^\circ - 280^\circ$.
- During **MY 34**, the observed **plume appears later**, with lower abundances above 80 km.
- We attribute this difference to **TGO spacecraft sampling** variations and to long-term effects of the MY 34 Global Dust Storm, leading to a possible **weakening of the southern Polar Vortex** [21] during the storm enhancing **dust deposition** over water ice reservoirs [22].
- We provide a rough **estimation of the hydrogen escape flux** associated to the strong plumes in MY35 and 36 of about $\sim 3.2 \pm 0.5 \times 10^9 \text{ cm}^{-2} \text{ s}^{-1}$ associated to the plumes, which adds to the importance of the perihelion season to the global budget of hydrogen escape on Mars.

Acknowledgments

The IAA/CSIC team acknowledges financial support from the Severo Ochoa grant CEX2021-001131-S and by grants PID2022-13759NB-I00, RTI2018-100920-J-I00 and PID2022-141216NB-I00 all funded by MCIN/AEI/10.13039/501100011033. A. Brines acknowledges financial support from the grant PRE2019-088355 funded by MCIN/AEI/10.13039/501100011033 and by 'ESF Investing in your future'. ExoMars is a space mission of the European Space Agency (ESA) and Roscosmos. The NOMAD experiment is led by the Royal Belgian Institute for Space Aeronomy (IASB-BIRA), assisted by Co-PI teams from Spain (IAA- CSIC), Italy (INAF-IAPS), and the United Kingdom (Open University). AM was supported by the Institute for Basic Science (IBS-R035-C1).



8 - 13 September 2024
Berlin, Germany

